Stochastic Dynamics Simulations of *n*-Alkane Melts Confined between Solid Surfaces: Influence of Surface Properties and Comparison with Scheutjens−Fleer Theory

T. Matsuda

Research and Development Center, UNITIKA Ltd., 23 Kozakura, Uji-shi, Kyoto, 611 Japan

G. D. Smith

Thermosciences Institute, STC 230-3, NASA Ames Research Center, Moffett Field, California 94035

R. G. Winkler

Abteilung Theoretische Physik Universität Ulm, Albert-Einstein-Allee 11, 7900 Ulm, Germany

D. Y. Yoon*

IBM Almaden Research Center, 650 Harry Road, San Jose, California 95120-6099

Received March 17, 1994; Revised Manuscript Received July 28, 1994®

ABSTRACT: Stochastic dynamics simulations of *n*-alkane melts ($C_{13}H_{28}$ and $C_{28}H_{58}$) confined between solid surfaces have been performed in order to study the influence of the surface structure and interactions on the structural and dynamic properties of the chain molecules at the interfaces. Moreover, these simulation results have been compared with the predictions of the Scheutjens−Fleer lattice theory in order to investigate the general applicability of the theory in predicting the conformational properties of real (atomistic) melt chains at the interfaces. The *n*-alkane chains are described as mass points (united atoms) linearly connected by rigid bonds and subjected to bond bending, torsional, and nonbonded interaction potentials. For repulsive surfaces, an atomistic, ordered surface was found to yield the same static and dynamic properties of the chains as a flat, structureless surface. The presence of a strongly attractive surface was found to increase layering of both monomers and entire *n*-alkane molecules at the surface. Chains with only ends strongly attractive to the surfaces (sticky ends) exhibited an increased probability of long tails and loops and a decreased probability of long trains. However, no significant change in the strong preference for trains comprised of entire molecules was seen. Comparison of neutral surface and sticky end simulations with Scheutjens−Fleer self-consistent-field lattice theory predictions revealed that the theory reproduces quite well the behavior of tails, loops, and trains seen from atomistic simulations of $C_{28}H_{58}$.

1. Introduction

Since understanding the behavior of chain molecules at an interface is of great importance in designing lubricants, polymer coatings, composite materials, etc., a number of experimental[1,2] and theoretical[3−14] studies have been performed on this subject. Among the many issues which still warrant investigation is the influence of surface properties on the behavior of the molecules at the interface.

On the theoretical side, both analytical models and simulation methods have been applied to obtain a fundamental understanding of chain conformations and dynamics of polymer melts confined by solid surfaces. Simulation studies have employed lattice chains,[4−6] bead chains,[7−9] and atomistic polymethylene chains of both united atoms[10−12] and explicit atoms.[13] In this regard, the consequence of various approximations adopted in the different methods has not been fully investigated. Specifically, one needs to understand how closely the results of atomistic models can be represented by simulations or theoretical methods employing coarse-grained chain models of lattices or beads. Recently, it was shown[14] that the Scheutjens−Fleer self-consistent-field theory[15] reproduces well the results of Monte Carlo simulations of cubic-lattice chains as demonstrated by the close agreement of predicted segmental packing and orientation as well as chain conformations at the interfaces of polymer melts confined by solid walls. A similar comparison of the predictions of the Scheutjens−Fleer theory with atomistic simulations results has not been carried out. Such a comparison on short chain systems, for which both the atomistic simulations and theoretical calculations can be carried out accurately, is critically needed in order to understand the limits of theoretical predictions for high molecular weight systems.

In this study we have performed a series of stochastic dynamics simulations of *n*-alkane ($C_{13}H_{28}$ and $C_{28}H_{58}$) melts confined between solid surfaces. In order to elucidate the dependence of the equilibrium and dynamic properties of the melts on surface properties, several aspects of the chain segment−surface interactions have been studied. First, we investigated the effect of the surface topography; the melt was confined between two stationary, atomic crystalline solid surfaces and stationary nonstructured smooth solid surfaces. Next, we investigated the effect of attraction between a surface and the chain segments by simulating systems with neutral purely repulsive surfaces, strongly attractive surfaces, and surfaces which are strongly attractive only to the chain ends (sticky ends).

® Abstract published in *Advance ACS Abstracts,* October 15, 1994.

0024-9297/95/2228-0165$09.00/0

In section 2 of the paper the systems and simulation method are described. The results for structural and dynamic properties are presented in section 3, followed by a comparison with the predictions of the Scheutjens–Fleer self-consistent-field lattice theory in section 4. Finally, section 5 summarizes our findings.

2. Systems and Simulation Methodology

We consider the n-alkane chains to be comprised of mass points, which represent CH_2 units (united atoms) with a mass of 14. Bond lengths are constrained to the experimental value of 0.153 nm. The valence angle between successive bonds is maintained close to an experimental value (θ_0) by a potential quadratic in cos θ

$$V(\theta) = \frac{k_\theta}{2}(\cos\theta - \cos\theta_0)^2 \tag{1}$$

where θ is the valence angle and θ_0 and k_θ were chosen to be 112° and 119.6 kcal/mol, respectively. The "one–four" interactions between units belonging to the same chain and separated by three skeletal bonds are included by the torsional potential[10]

$$V(\phi) = \frac{k_\theta}{2}\{x(1 - \cos\phi) + (1 - x)(1 - \cos 3\phi)\} \tag{2}$$

The parameters for this potential were $k_\phi = 4.1$ kcal/mol and $x = 0.163$.[10] These values yield 0.5 and 3.6 kcal/mol for the energy difference and the barrier height, respectively, between the trans and the gauche states.

Finally, nonbonded interactions between units of different chains and units belonging to the same chain at least four bonds apart from each other are given by a shifted and truncated Lennard-Jones potential

$$V(r) = \begin{cases} \epsilon\left(\left(\frac{\sigma}{r}\right)^{12} - 2\left(\frac{\sigma}{r}\right)^{6} + 1\right) & \text{for } r \le \sigma \\ 0 & \text{for } r > \sigma \end{cases} \tag{3}$$

where r is the distance between the united atoms. The parameters of the Lennard-Jones potential are $\epsilon = 0.14$ kcal/mol and $\sigma = 0.4$ nm.

Neutral Surfaces. The polymeric chains were confined between parallel surfaces. For one case, a crystalline (structured) surface was assumed. The interaction of a monomer with the surface was chosen to be the same as for the monomer–monomer interaction; i.e., the potential of eq 3 was used. For another case, we assumed a structureless, flat, purely repulsive surface. A potential for this flat surface is obtained by considering the solid underneath the surface to be a continuum and by integrating the continuous interaction potentials of the points of the solid over its volume. Assuming the surface to be composed of closed-packed atoms, representing a (111) face of a face-centered-cubic (fcc) solid, the potential was integrated over the interaction range σ. Consequently, we obtained the potential

$$V_F(z) = \begin{cases} \frac{\pi}{3}\varrho\sigma^3\epsilon\left(\frac{1}{15}\left(\frac{\sigma}{z}\right)^9 - \left(\frac{\sigma}{z}\right)^3 + \left(\frac{z}{\sigma}\right)^3 - \frac{54}{10}\left(\frac{z}{\sigma}\right) + \frac{16}{3}\right) & \text{for } z \le \sigma \\ 0 & \text{for } z > \sigma \end{cases} \tag{4}$$

In the calculation of V_F the surface is assumed to be at $z = 0$. The density ϱ of the solid was chosen to be $\varrho = 2^{1/2}/\sigma^3$. This is the density of a fcc lattice with a lattice spacing of $2^{1/2}\sigma$. The potential (eq 4) is different from a 9–3 Lennard-Jones potential for a nontruncated interaction.[16] It is more repulsive due to the missing attraction of the next layers in the solid. A detailed investigation[16] shows that eq 4 does not give a good approximation of the original structured surface. Though the minimum of the potential is not shifted, it is less repulsive than the original potential for most of the points on the surface. (Strictly speaking, the above approximation is just valid near the potential minimum, i.e., near $z = \sigma$.)

Attractive Surfaces. In addition to the purely repulsive Lennard-Jones type potential (we call this a neutral surface in the present study), an attractive potential was also employed in order to investigate the effect of attractive interactions between a surface and the chain segments. Assuming the potential between a point charge and a flat metal surface to be proportional to the inverse of the distance between the point and the surface, we employed the following simple form of an attractive potential

$$V_{sp} = -\frac{\epsilon_{sp}}{z}s(z) \tag{5}$$

where

$$s(z) = 1 - 10\left(\frac{z}{z_c}\right)^3 + 15\left(\frac{z}{z_c}\right)^4 - 6\left(\frac{z}{z_c}\right)^5 \tag{6}$$

z is the distance between a monomer and the flat surface. The polynomial function $s(z)$ is such that the potential smoothly levels off at the truncation distance z_c. The factor ϵ_{sp} and the truncation distance z_c were chosen to be 50 kcal·nm/mol and 0.8 nm, respectively. This form of the function with the above parameters corresponds to the interaction of a particle charged with 0.25 eu and a flat metal surface. We expect that structural properties of a polymeric melt are not very sensitive to the particular form of the attractive potential. Instead of eq 5 an attractive 9–3 Lennard-Jones potential with the same energy minimum was also applied and was found to lead to the same qualitative behavior. Therefore, in the course of this study, this attractive function will be applied to all monomers (attractive surface) or only chain ends (sticky ends).

Stochastic Dynamics. The equations of motion of a chain are given by the Langevin equations[17,18]

$$m_i\ddot{\mathbf{r}}_i = \mathbf{F}_i + \mathbf{F}'_i - \gamma m_i\dot{\mathbf{r}}_i + \Gamma_i \tag{7}$$

where $\mathbf{F}_i$ denotes the forces due to the potentials (eqs 1–5) and the vector $\mathbf{F}'_i$ the forces of constraint

$$\mathbf{F}'_i = \lambda_{i-1}(\mathbf{r}_i - \mathbf{r}_{i-1}) - \lambda_i(\mathbf{r}_{i+1} - \mathbf{r}_i) \tag{8}$$

induced by the constraint of bond lengths

$$l^2 = (\mathbf{r}_i - \mathbf{r}_{i-1})^2 \tag{9}$$

where the λ's are Lagrangian multipliers and l is the bond length. The stochastic force Γ_i is assumed to be stationary, purely random, and Gaussian (white noise):

$$\langle\Gamma_i(t)\rangle = 0 \tag{10}$$

$$\langle\Gamma_{i\alpha}(t)\,\Gamma_{j\beta}(t')\rangle = 2k_B T\gamma m_i\delta_{ij}\delta_{\alpha,\beta}\delta(t-t') \tag{11}$$

with T the temperature of the system. The indices α and β denote the Cartesian components of the force. This type of equation keeps the temperature fixed rather than the energy. Additionally, the Fokker–Planck equation corresponding to eqs 7–11 can be numerically solved. The stationary solution of this equation is the Boltzmann distribution,[17,18] Thus, stochastic dynamics simulations produce canonical time averages. However, due to the additional damping in the system (via a background heatbath) dynamic quantities are changed depending on their relaxation rate and the damping by the bath. In order to extract the correct time behavior of a dynamic quantity, $1/\gamma$ has to be chosen larger than the relaxation time of the quantity. However, on that shorter time scale no longer a canonical ensemble is simulated. We chose $1/\gamma = 750$ fs in this study, which was found to be satisfactory in previous studies.[12,13] For integration of the equations of motion we used a method proposed by van Gunsteren and Berendsen.[19] The calculation of the Lagrangian multipliers (eq 8) was done by a method similar to the SHAKE[20] algorithm which takes advantage of the fact that only the nearest neighbors along the chains interact.[21] The integration time step was chosen to be 3.7 fs. We investigated two systems of different chain lengths, namely, a melt of *n*-tridecane ($C_{13}H_{28}$) chains at 300 K and of *n*-octacosane ($C_{28}H_{58}$) chains at 400 K.

Simulation Systems. The *n*-alkane chains are confined between solid surfaces parallel to the *xy* plane. In the *x* and *y* direction periodic boundary conditions were applied. The separation of the two surfaces was chosen to be 3.0 nm for the tridecane system and 3.5 nm for the octacosane system. The size of the periodic *xy* planes was set to $2.8 \times 1.6\sqrt{3}$ nm for the tridecane and $3.2 \times 2.0\sqrt{3}$ nm for the octacosane system. The simulation box contained 49 tridecane chains and 40 octacosane chains, respectively, yielding experimental melt densities[22] at the given temperatures in the middle of the films. The initial coordinates of tridecane and octacosane melts were first generated by the method described in ref 10 between flat surfaces. In this method the first monomer of a chain is randomly generated in the simulation box and successive monomers are generated with fixed bond lengths $l = 0.153$ nm and bond angles $\theta = 112°$ varying the torsional angles in accordance with random numbers, where no two monomers except for a covalently connected pair can be closer than 0.24 nm. These high energy coordinates were relaxed by the stochastic dynamics run of 7.5 ns. Next, this relaxed system was further equilibrated for 3.7 ns. Finally, the properties, which we will discuss in the following section, were calculated at each integration time step and averaged over the sampling simulation period of 7.5 ns. The mean-square end-to-end distances were monitored during the sampling simulation period. No practical change except for statistical improvement was observed during the sampling period, and symmetric profiles with respect to the center of the film were obtained.

3. Results and Discussion

Effect of Surface Topography. First, we studied the influence of the surface topography, i.e., the structure of the surface, on the melt. We simulated two systems of tridecane melts at 300 K: one confined between flat smooth surfaces and the other one between structured surfaces as described in the previous section. Tridecane melts confined between flat surfaces were investigated first by Vacatello et al.[10] using a Monte Carlo method, and recent results from stochastic dynamics simulations[12] were in perfect agreement with theirs. In this study our main interest was to determine whether the use of structured surfaces results in significant changes in chain conformations and dynamics, due to effects such as epitaxial crystallization.

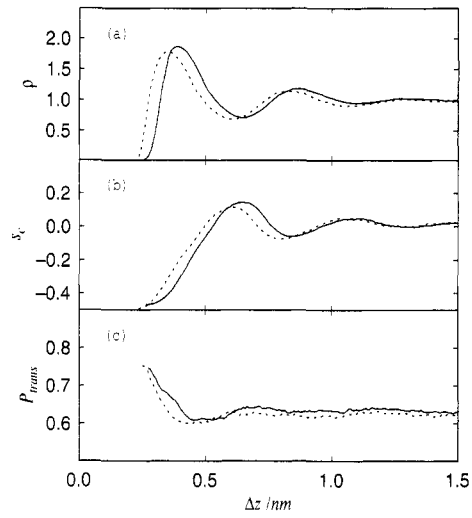

Figure 1. Monomer densities (a) as a function of the distance from the surface, the two-bond segment order parameters (b) defined by eq 12 as a function of the distance between the surface and the center of mass of a two-bond segment, and the fractions of trans bonds (c) as a function of the distance between the surface and the center of mass of four monomers. The system contained tridecane chains at 300 K confined between flat surfaces (dotted lines) and structured surfaces (solid lines). The monomer densities are normalized with respect to the experimental bulk density.

The profile of the local structures is shown in Figure 1, where the dotted lines correspond to the system with flat surfaces and the solid lines to the system with structured surfaces. The monomer densities are plotted in Figure 1a as a function of the separation from one of the surfaces. The values were normalized with respect to the experimental bulk density. The shape of the density curve is practically the same for both systems, except that the positions of the maxima and minima differ by approximately 0.03 nm. As mentioned in the previous section, the flat potential is a rather crude approximation of the crystalline surface. The averaging process which accompanies the continuum description makes the flat surface less repulsive compared to various points on a structured surface.[16] Thus, it is not surprising that the profiles of Figure 1 are shifted slightly relative to each other.

Information on chain orientation is given by the order parameters s_c of two-bond segments, formed by three covalently connected monomers, with respect to the *z* axis. The order parameter is defined as

$$s_c = \frac{1}{2}\langle 3\cos^2\theta_c - 1\rangle \qquad (12)$$

where θ_c is the angle between the *z* axis and the vector connecting two monomers separated by two bonds. The results are plotted in Figure 1b as a function of the distance between the center of mass of the two-bond segments and the surfaces. Since the monomer density is shifted toward the middle of the film for the structured surface system, the profile of the order parameter is also shifted. Aside from that, the profiles for the different surface structures are practically identical. The

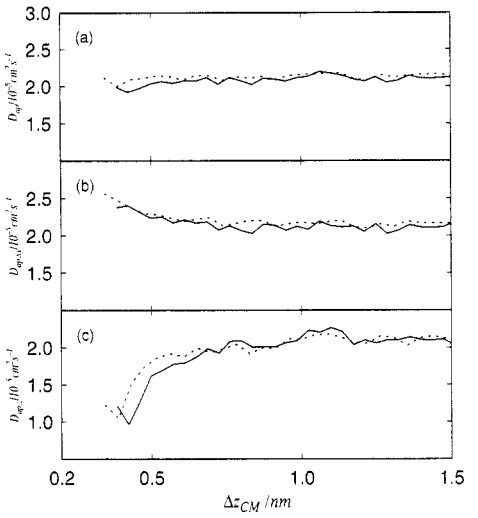

Figure 2. Apparent diffusion constant (a) defined by eq 13 of a tridecane melt at 300 K, its xy componet multiplied by 1.5 (b), and its z component multiplied by 3 (c) as a function of the distance between the surface and the center of mass of a molecule. Dotted lines correspond to the flat surface system and solid lines to the structured surface system.

chain segments are significantly oriented parallel to the surface adjacent to the surfaces in both systems. But this orientation is less pronounced at the farther separations. For a more detailed discussion see ref 12.

The fraction of bonds in the trans conformation is defined as the probability of bonds with torsional angles between −60° and +60°. The dependence of this quantity on the separation between one of the surfaces and the center of mass of the four monomers defining a torsional angle is shown in Figure 1c. Except for the shift of the curves, the chain conformations are practically the same for both systems. Therefore, it is clear that the ordered surface structure has little effect on the local chain configurations of chain molecules; i.e., no epitaxial effects are seen. This finding is in good agreement with the results of Monte Carlo simulations by Vacatello and Aurieman.[23]

We also investigated the dynamic properties of the chains in the different systems via the apparent diffusion constant defined by

$$D_{ap} = \frac{1}{6t_c}\langle(\mathbf{r}_{cm}(t + t_c) - \mathbf{r}_{cm}(t))^2\rangle \qquad (13)$$

where t_c was chosen to be 750 fs and $\mathbf{r}_{cm}$ represents the position of the center of mass of a molecule. The average was taken over different times and chains. In Figure 2 we plot the apparent diffusion constant (a), its xy component (b), and its z component (c), where dotted lines denote the results for the flat surface system and solid lines are for the structured surface system. Within the precision of the calculation no change in the mobility is found.

Effect of Attractive Surfaces. The effect of an affinity between a surface and the confined molecules was investigated by including an attractive function in the interaction potential of the surface and monomers. We call this an attractive surface. As shown in the last section, a surface corrugation did not change any of the equilibrium or dynamic properties investigated for the neutral surfaces. Therefore, the current study is restricted to the case of flat surfaces. Figure 3 shows the Lennard-Jones potential for the flat surface (eq 4)

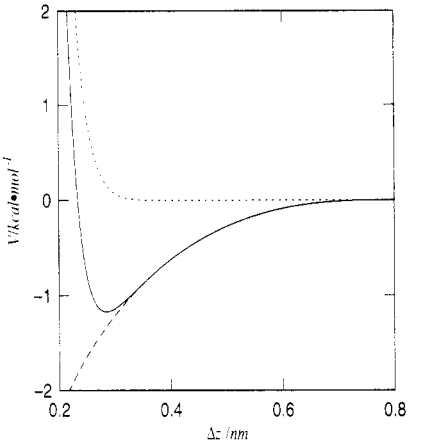

Figure 3. Potential energy of an attractive surface. The dotted line represents the Lennard-Jones potential (eq 4) for the flat surface, the dashed line represents the attractive part (eq 5), and the solid line is for the resulting potential.

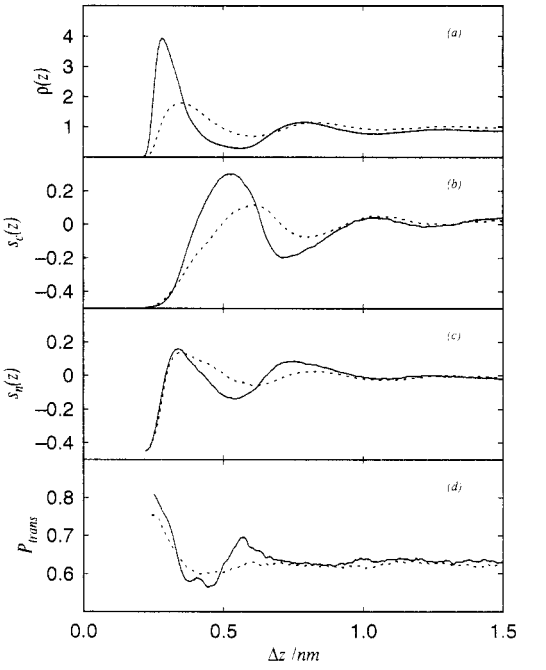

Figure 4. Monomer densities (a) as a function of the distance from the surface, the two-bond segment order parameters (b), defined by eq 12, its complementary order parameter (c) (see text) as a function of the distance between the surface and the center of mass of a two-bond segment, and the fraction of trans bonds (d) as a function of the distance between a surface and the center of mass of four monomers in a tridecane melt at 300 K confined between neutral (dotted line) and attractive (solid line) surfaces. The monomer densities are normalized with respect to the experimental bulk density.

(dotted line), the introduced attractive interaction (dashed line), and the overall potential (solid line). The minimal potential energy is −1.2 kcal/mol. Compared to the Lennard-Jones parameter ϵ = 0.14 kcal/mol, this potential is strongly attractive. Hentschke et al.[24] calculated the surface potential between a graphite surface and a $C_{24}H_{50}$ molecule by Steele's method[16] and obtained a potential with a minimal energy of approximately −40 kcal/mol per chain, i.e., −1.7 kcal/mol per monomer. Thus, our surface with the attractive potential is somewhat less attractive than a graphite surface. For the attractive surfaces we simulated a tridecane melt at 300 K.

The monomer density profile is shown in Figure 4a. In each part of Figure 4, the dotted line corresponds to

the result for the surfaces with Lennard-Jones potentials only (neutral surface), and the solid line, to the one for the attractive surfaces. One can see a significant increase in the monomer density adsorbed on the attractive surface. The maximum of the density is observed at $z = 0.30$ nm, close to the potential minimum, $z = 0.29$ nm. This enhanced density at the surface is followed by a deep depletion region and then the second maximum.

We also calculated the orientational order parameter of the two-bond segment s_c defined by eq 12 and the complementary order parameter s_n calculated from the same equation replacing θ_c by θ_n, where θ_n is the angle between the z axis and the vector perpendicular to the direction of the two-bond segment and contained in the plane of the segment. These are shown in parts b and c of Figures 4, respectively. At the density maximum near the attractive surface, the order parameters s_c is close to its minimal value, indicating almost perfect orientation along the surface plane. Such an alignment is found to be considerable even at the second density maximum in the system with attractive surfaces, while it is less pronounced in the system with neutral surfaces. In the depletion region between the adsorbed layer and the second maximum, the net orientation is perpendicular to the surfaces, especially for the attractive surface system. The complementary order parameters s_n is approximately equal for the attractive and neutral surface systems within the adsorbed layer. At the density maximum of this layer near the attractive surface s_n is slightly smaller than zero. At slightly greater distances, but within the adsorbed layer, s_n is somewhat greater than zero, indicating a tendency of two-bond segment planes to orient toward the normal direction to the surfaces. This tendency is also seen for the segments in the region of the second density maximum for the attractive surfaces.

The fraction of trans bonds is plotted in Figure 4d as a function of the separation distance between a surface and the center of mass of four monomers. As the figure shows, the number of bonds in the trans state is moderately increased in the adsorbed layer. In the case of the neutral surfaces, the fraction of bonds in the trans state at the maximum of the monomer density is similar to the bulk value, whereas for the attractive surfaces this fraction is increased. Thus, the chains in the adsorbed layer are more extended for the attractive surface system.

Figure 5 shows the density of molecular mass center (a) and mean-square radius of gyration, $\langle r_g^2 \rangle$ (b; upper curve), and its z component, $\langle r_{gz}^2 \rangle$ (b; lower curve), where dotted lines denote the system with neutral surfaces and solid lines the system with attractive surfaces. Like the monomer density, the density of centers of mass is also drastically changed when the chain segments are attracted to the surfaces. The peak of the centers of mass in the system with attractive surfaces is located at a separation of approximately 0.3 nm from the surface with a peak height 6 times greater than the bulk value. This separation coincides with the potential minimum. Moreover, a broad and deep region of depleted mass center density follows. Then, another peak of smaller height can be observed. The attraction by the surface drastically influences the overall shape of the molecules. This is reflected by the radius of gyration. In the middle of the film none of its components is favored in the average; i.e., the chain configuration is isotropic. For those chains whose center of mass is located in the

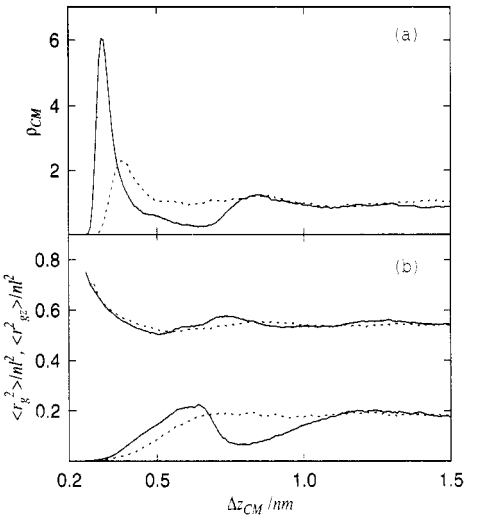

Figure 5. Normalized density of center of mass (a), the mean-square radius of gyration (b; upper curves) and its z component (b; lower curves) as a function of the separation between the molecular mass center and the nearest surface in the system of tridecane melts at 300 K confined between neutral surfaces (dotted lines) and attractive surfaces (solid lines).

region of the second mass center maximum (0.8 nm), the z component decreases. However, the total radius of gyration is practically unchanged. Consequently, the main axes of the chains align themselves parallel to the surfaces. At the mass center density maximum near the surface the radius of gyration becomes larger than the bulk value, while $\langle r_{gz}^2 \rangle$ decreases toward zero, as expected. Thus, there is a large number of chains with all the segments confined within the monolayer near the attractive surface. Our results are therefore in good agreement with the recent work of Ribarsky and Landman.[11]

Previously, we studied in detail the shape of molecules close to the surface, adapting the concept of train, tail, and loop sequences to an off-lattice system.[12] In this study we considered a bond as a unit element and formulated the following definitions:

(1) The thickness of the interface is chosen to be 0.7 nm.

(2) Trains are successive bonds in the interface.

(3) Tails are sequences of bonds which contain chain ends located outside the interface and the other end of the sequence connected to a monomer within the interface.

(4) Loops are sequences of bonds which are out of the interface, with both ends of the sequences connected to monomers in the interface.

(5) If a train connects to a tail or loop, the division point is defined by the orientation of the last bond belonging to the interface. If the angle between the z axis and the axis defined by the last two bonds is smaller than 45°, the last bond of this train is switched to a tail or loop.

The frequency of the occurrence of train, tail, and loop sequences was counted and averaged over the simulation period, and the weighted probability was calculated, defined by

$$P(i) = f(i)\, i/N \tag{14}$$

where N is the total number of bonds in the simulation box and $f(i)$ is the number of sequences of i bonds in length. Thus, $P(i)$ corresponds to the probability of a bond observed in a certain sequence of length i.

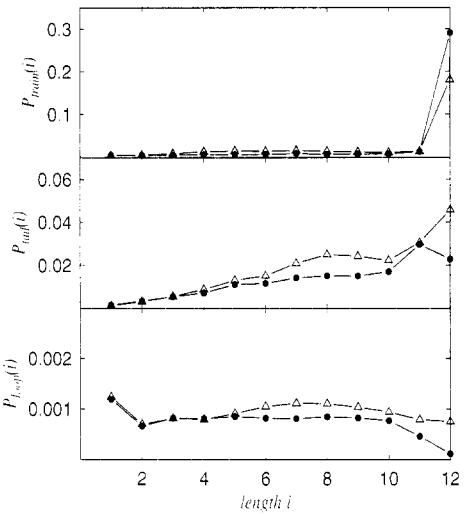

Figure 6. Probability distribution of trains (a), tails (b), and loops (c) defined by eq 14 found in tridecane melts at 300 K in a system of neutral surfaces (triangles) and of attractive surfaces (circles).

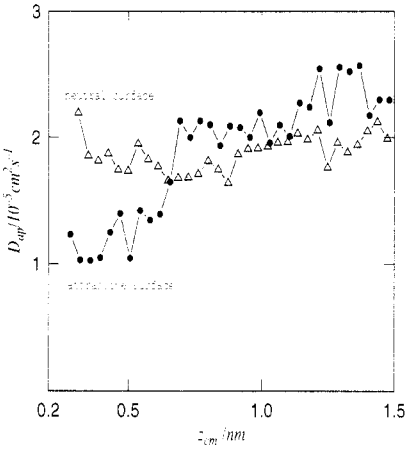

Figure 7. Apparent diffusion constant defined by eq 13 as a function of the distance between the surface and the center of mass of a molecule in a system of tridecane melts at 300 K confined between the neutral surfaces (triangles) and the attractive surfaces (circles).

The results for the neutral and attractive surface systems are plotted in Figure 6. The probability of trains involving entire tridecane chains (i = 12) is strongly enhanced by the attractive surface (a). This enhancement reflects the greater chain mass center density found in the adsorbed layer for the attractive surface system (see Figure 5a) and indicates that monomer segments near the attractive surface participate to a larger extent in two-dimensional chain configurations. This two-dimensional structure is also supported by the reduction in the occurrence of short trains as well as the decrease in long tail and loop sequences for the attractive surface system.

Figure 7 shows the apparent diffusion constants calculated by eq 13 for both systems. In the neutral surface system, the apparent diffusion constant is independent of the distance from the surface as a result of a reduced mobility perpendicular to the surface and enhanced mobility along the surface, as reported in the previous study.[12] In contrast, the diffusion constant near an attractive surface decreases substantially, and the diffusivity parallel to the surface is also reduced. The reduction of the mobility normal to the surface can be attributed to the stronger restriction by the attractive surface. The reduced mobility parallel to the surface

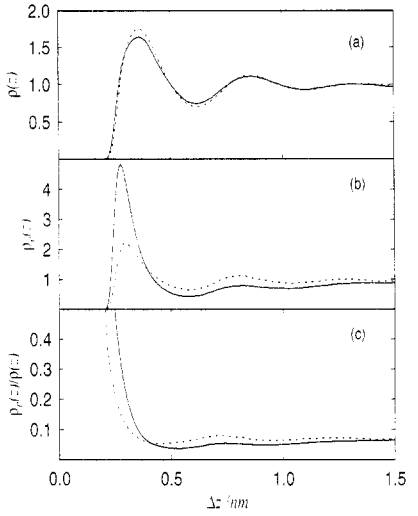

Figure 8. Monomer densities (a) normalized with respect to the bulk density, the densities of chain ends (b) normalized with respect to the bulk value, and the inverse ratio of the above densities (c) as a function of the separation from a surface found in an octacosane melt at 400 K. Dotted lines denote the system with neutral surfaces and solid lines that with sticky ends.

is most likely due to the enhanced density and thus reduced free volume near the surface, as pointed out by Mansfield and Theodorou to explain their dynamic Monte Carlo simulation results.[6]

It should be noted that, because our simulations were performed at constant density, the monomer density toward the center of the film with the attractive surfaces is slightly reduced from the bulk value which was obtained for the neutral surfaces, as illustrated in Figure 4a. This is a result of the increase in monomer density near the attractive surfaces. If the simulations of the system with attractive surfaces were performed at constant chemical potential (given by the system with neutral surfaces), it could be expected that the monomer density overall would increase slightly through the inclusion of additional chains to the point where the density in the center of the film was the same as that for the neutral surfaces. Such an effect would not change the trends seen in segment properties (distribution and orientation) and chain properties (distribution, conformations, dimensions, and dynamics) seen in going from neutral to attractive surfaces. Quantatively, the effect of the surfaces might be expected to be somewhat greater for a comparison at constant chemical potential as the change in the monomer density at the surface, which influences many of these properties, would be slightly greater than for the constant density case.

Effect of Sticky Ends. Next, we investigated the effect of sticky ends. Since tridecane chains are considered rather too short to exhibit significant loop configurations, we chose octacosane melt at 400 K. We applied the attractive potential only to the chain ends (sticky ends) of octacosane chains, while the Lennard-Jones potential (eq 4) is applied to the internal monomers. Figure 8 shows the density of monomers (a), chain ends (b), and the inverse ratio of these two quantities (c) as a function of the distance from the surface. In each part, the dotted line represents the neutral system and the solid line the system with sticky ends to the surface. Even in the neutral system, chain ends prefer to stay closer to the surface than the internal monomers, as has also been observed in previous studies.[7-10] In the system with sticky ends, the

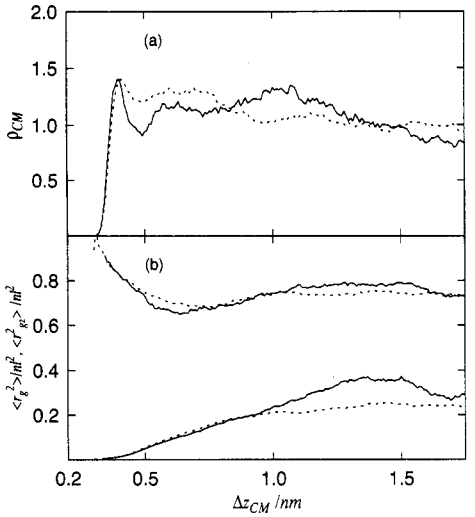

Figure 9. Normalized density of centers of mass (a), the mean-square radius of gyration (b; upper curves), and their z components (b; lower curves) as a function of the separation between molecular mass center and the nearest surface of octacosane melts at 400 K. Dotted lines denote the system with neutral surfaces and solid lines that with sticky ends.

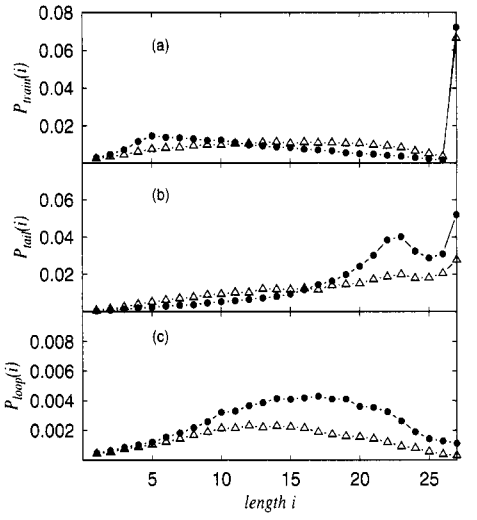

Figure 10. Probability distribution of trains (a), tails (b), and loops (c) defined by eq 14 found in the systems of octacosane melts at 400 K with neutral surfaces (triangles) and sticky ends (circles).

density of chain ends adjacent to the surface increases significantly, while in the following region a deep depletion is observed. Moreover, the maximum of the monomer density near the surface is lower than that for the neutral system. This is explained by a partial destruction of the preferential two-dimensional alignment of chains by the enhanced number of chain ends at a surface in the sticky end system, as discussed below.

Figure 9 shows the density of center of mass (a), the mean-square radius of gyration (b; upper curves), and its z component (b; lower curves) as a function of the separation from the surface. In each part the dotted line denotes the system with neutral surface and the solid line the system with sticky ends. The center of mass densities for both systems show a weak peak adjacent to the surface (Δz of around 0.4 nm). In the system with sticky ends this first peak is narrower and is followed by a deeper depletion region and a second weak, broad peak. It should also be noted that the z component of the radius of gyration in the system with sticky ends increases significantly at Δz of around 1.4 nm. This reflects the fact that chains in this region mainly belong to long tails and loops.

We also calculated the probability of trains, tails, and loops, which are plotted in Figure 10. The increase of shorter trains and the decrease of longer trains are observed in the sticky end system. This may be attributed to the increased number of chain ends close to the surface which somewhat exclude internal monomers. Thus, longer trains are replaced by short trains which connect to long tails and, to a lesser extent, loops, as can be seen in parts b and c of Figure 10. However, the probability of trains involving entire $C_{28}H_{58}$ molecules ($i = 27$) remains the same. In the previous study,[12] it was observed that the interface is composed of many long trains, which often involve entire $C_{28}H_{58}$ molecules and chain ends. Here it is seen that this feature of the interface remains even if the chain ends are modified to be sticky to a surface. This picture agrees with the profile of the density of center of mass (Figure 9a); the first narrow peak is consistent with the presence of a significant number of chains completely adsorbed on the surface, while the depletion region and the following broad second peak are consistent with the presence of long tails.

4. Comparison with the Scheutjens–Fleer Lattice Theory

The behavior of loops, tails, and trains seen here for $C_{28}H_{58}$ chains for the neutral and sticky end systems is predicted by the Scheutjens–Fleer self-consistent-field (SCF) lattice theory. Examples for loops and tails can be seen in ref 14. For trains, we have attempted to perform calculations on a system which models the octacosane system studied here. The system consisted of a 90% filled cubic lattice consisting of seven layers (layers 1 and 7 being the surface layers), consistent with the seven monomer density peaks observed in the $C_{28}H_{58}$ system, with each layer corresponding to the dimensions of about 4.5 Å observed between monomer density peaks (see Figure 12). An occupancy of 90% was chosen for the lattice to allow for differences in density between the layers. Results for a 50% filled lattice showed no significant differences from the 90% filled lattic. The chains were 8 segments in length since a lattice segment of about 4.5 Å corresponds to around 3.5 CH_2 monomer units. The attractive energy for the end segments to the surfaces was set at 1 kcal/mol, and calculations were performed at 400 K. The reader is referred to ref 14 and the references contained therein for details of the SCF calculations. The resulting train probabilities are compared with simulation results in Figure 11, where a surprisingly good agreement between simulations and SCF lattice predictions can be seen. The decrease in the number of long trains and the increase in the number of short trains for the sticky end system are reflected in the SCF calculations. The dramatic increase in the probability of a train consisting of an entire chain (length n) with respect to a train of length $n - 1$ is also predicted by the SCF calculations, as is the fact that the probability of a train of length n is not significantly changed by the presence of sticky ends. For the SCF lattice calculations with the neutral surface, the increase in the probability of a train of length n relative to a train of length $n - 1$ is simply the result of the fact that there are more lattices sites available on the surface for the nth unit (4) than off the surface (1). For the case of sticky ends, the probability of the nth unit being on the surface is dramatically

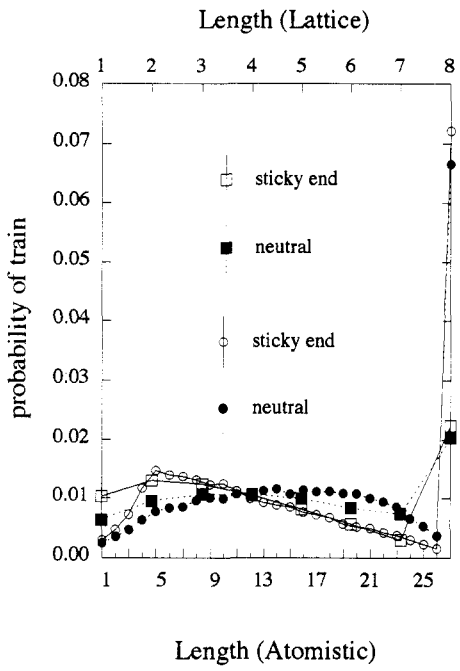

Figure 11. Probability distribution of trains for octacosane melts at 400 K with neutral surfaces and sticky ends, compared to SCF lattice theory predictions (squares). The SCF probabilities have been scaled by (8/27) for comparison.

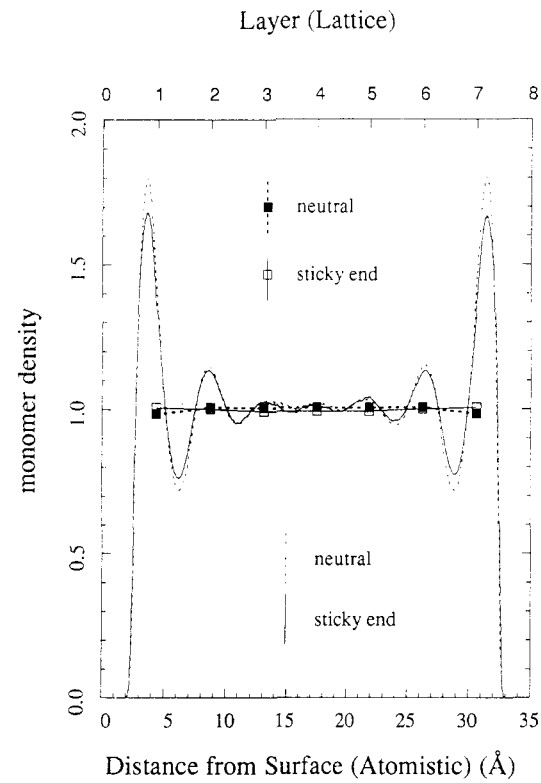

Figure 12. Monomer density profile for octacosane melts at 400 K with neutral surfaces and sticky ends, compared to SCF lattice theory predictions (squares). The monomer densities are normalized with respect to the bulk values.

increased by the attractive energy, but as the probability of long train sequences is reduced by the higher concentration of chain ends on the surface, the net result is that the probability of a train of length n is not significantly affected by the attractive potential.

To some extent the good agreement for the train distributions between the atomistic simulations and the SCF lattice predictions for longer trains is the result of the canceling of errors: The backfolding nature of random-walk SCF lattice chains tends to increase the probability of longer trains (compared to self-avoiding chains[14]), while the lower persistence of the SCF lattice chains (compared to atomic chains) tends to decrease the probability of longer trains.

Although the SCF lattice theory qualitatively reproduces chain conformations, the lattice model by nature is incapable of predicting features which occur on a length scale smaller than the lattice spacing. For example, the detailed oscillations in the monomer distribution profile, which occur on a monomer length scale, cannot be reproduced by the lattice model. This is demonstrated in Figure 12, where the monomer distribution profiles for octacosane from simulation and SCF lattice theory are compared. However, on the length scale of the lattice spacing the monomer density profile, given as the average monomer density within each layer, as determined from our simulations shows little structure, in agreement with the SCF lattice predictions.

5. Conclusions

Stochastic dynamics simulations of n-alkane melts $C_{13}H_{28}$ and $C_{28}H_{58}$ confined between solid surfaces of various nature were performed. We investigated the influence of the surface structure on the equilibrium and dynamic properties of the chains. Two different surface structures were considered: a crystalline solid surface and a flat (structureless) solid surface. Moreover, we simulated the behavior of the chains in the vicinity of strongly attractive surfaces and compared the results with those of purely repulsive surfaces. Finally, the structural properties were analyzed for a system with attractive chain ends (sticky ends).

The chain configurations and mobility are found to be rather insensitive to the atomistic topography or roughness of the surface for neutral surfaces. When the affinity between the chains and the surface was enhanced in the tridecane system, many chains are adsorbed on the surface assuming a more extended two-dimensional (layered) form. In the case of the octacosane chains with sticky chain ends to the surface, the number of longer tails and loops is increased. However, the high probability of entirely adsorbed train molecules on the surface is not affected. These conformational features are reproduced quite well by the Scheutjens–Fleer SCF lattice theory.

Acknowledgment. We express our thanks to Prof. M. Vacatello for helpful discussions and also UNITIKA Ltd. for financial support to T.M.

References and Notes

(1) Christenson, H. K.; Gruen, D. W. R.; Horn, R. G.; Israelachvili, J. N. *J. Chem. Phys.* **1987**, *87*, 1834.
(2) Van Alsten, J.; Granick, S. *Phys. Rev. Lett.* **1988**, *61*, 2570.
(3) Theodorou, D. N. *Macromolecules* **1988**, *21*, 1400.
(4) Madden, W. G. *J. Chem. Phys.* **1987**, *87*, 1405.
(5) Ten Brinke, G.; Aussere, D.; Hadziiounnou, G. *J. Chem. Phys.* **1988**, *89*, 4374.
(6) Mansfield, K. F.; Theodorou, D. N. *Macromolecules* **1989**, *22*, 3143.
(7) Kumar, S. K.; Vacatello, M.; Yoon, D. Y. *J. Chem. Phys.* **1988**, *89*, 5206.
(8) Kumar, S. K.; Vacatello, M.; Yoon, D. Y. *Macromolecules* **1990**, *23*, 2189.
(9) Bitsanis, I.; Hadziioannou, G. *J. Chem. Phys.* **1990**, *92*, 3827.
(10) Vacatello, M.; Yoon, D. Y.; Laskowski, B. C. *J. Chem. Phys.* **1990**, *93*, 779.

(11) Ribarsky, M. W.; Landman, U. *J. Chem. Phys.* **1992**, *97*, 1937.
(12) Winkler, R. G.; Matsuda, T.; Yoon, D. Y. *J. Chem. Phys.* **1993**, *98*, 729.
(13) Yoon, D. Y.; Smith, G. D.; Matsuda, T. *J. Chem. Phys.* **1993**, *98*, 10037.
(14) Smith, G. D.; Yoon, D. Y.; Jaffe, R. L. *Macromolecules* **1992**, *25*, 7011.
(15) Scheutjens, J. M. H.; Fleer, G. J. *J. Phys. Chem.* **1979**, *83*, 193.
(16) Steele, S. A. *The Interaction of Gases with Solid Surfaces*; Pergamon Press: Oxford, U.K., 1974.
(17) Risken, H. *The Fokker–Planck Equation*; Springer: Berlin, 1984.
(18) van Kampen, N. G. *Stochastic Processes in Physics and Chemistry*; North-Holland: Amsterdam, The Netherlands, 1981.
(19) van Gunsteren, W. F.; Berendsen, H. J. C. *Mol. Phys.* **1982**, *45*, 637.
(20) Ryckaert, J. P.; Ciccotti, G.; Berendsen, H. J. C. *J. Comput. Phys.* **1974**, *23*, 327.
(21) Winkler, R. G. Ph.D. Thesis, University of Ulm, Ulm, FRG, 1989.
(22) Doolittle, A. K.; Peterson, R. H. *J. Am. Chem. Soc.* **1951**, *73*, 2145.
(23) Vacatello, M.; Aurieman, F. *Makromol. Chem. Theory Simul.* **1993**, *2*, 77.
(24) Hentschke, R.; Schürmann, B. L.; Rabe, R. P. *J. Chem. Phys.* **1992**, *96*, 6213.